0888-8809/02/$15.00/0
Printed in U.S.A.

Molecular Endocrinology 16(2):390–401

Nuclear Transport of Parathyroid Hormone (PTH)-Related Protein Is Dependent on Microtubules

MARK H. C. LAM*, RACHEL J. THOMAS*, KATE LAKOSKI LOVELAND, STEVEN SCHILDERS, MIN GU, T. JOHN MARTIN, MATTHEW T. GILLESPIE, AND DAVID A. JANS

Nuclear Signaling Laboratory, Division of Biochemistry and Molecular Biology (M.H.C.L., D.A.J.), John Curtin School of Medical Research, Canberra, ACT 2601; Department of Biochemistry and Molecular Biology (M.H.C.L., D.A.J.), Monash University, Clayton, Victoria 3168; St. Vincent's Institute of Medical Research (R.J.T., T.J.M, M.T.G.), Fitzroy, Victoria 3065; Institute of Reproduction and Development (K.L.L.), Monash Medical Centre, Clayton, Victoria 3168; Centre for Micro-Photonics (S.S., M.G.), School of Biophysical Sciences and Electrical Engineering, Swinburne University of Technology, Hawthorn, Victoria 3122, Australia

PTH-related protein (PTHrP) was first discovered as a circulating factor secreted by certain cancers and is responsible for the syndrome of humoral hypercalcemia of malignancy induced by various tumors. The similarity of its N terminus to that of PTH enables PTHrP to share the signaling properties of PTH, but the rest of the molecule possesses distinct functions, including a role in the nucleus/nucleolus in reducing apoptosis and enhancing cell proliferation. PTHrP nuclear import is mediated by importin β1. In this study we use the technique of fluorescence recovery after photobleaching to demonstrate the ability of PTHrP to shuttle between cytoplasm and nucleus and to visualize directly the transport of PTHrP into the nucleus in living cells. Endogenous and transfected PTHrP was demonstrated to colocalize with microtubule structures *in situ* using various high-resolution microscopic approaches, as well as in *in vitro* binding studies, where importin β1, but not importin α, enhanced the microtubular association of PTHrP with microtubules. Significantly, the dependence of PTHrP nuclear import on microtubules was shown by the inhibitory effect of pretreatment with the microtubule-disrupting agent nocodazole on nuclear-cytoplasmic flux. These results indicate that PTHrP nuclear/nucleolar import is dependent on microtubule integrity and are consistent with a direct role for the cytoskeleton in protein transport to the nucleus. (*Molecular Endocrinology* 16: 390–401, 2002)

CONVENTIONAL NUCLEAR LOCALIZATION sequence (NLS)-mediated nuclear protein import initially involves the recognition of NLS-bearing proteins by the importin α/β1 heterodimer, followed by the docking of the complex to the nuclear pore and energy-dependent translocation into the nucleus mediated by the monomeric GTP-binding protein Ran and regulatory factors (1–3). Recent progress suggests a plethora of additional but analogous Ran-dependent nuclear transport pathways mediated by homologs of importin β1 (4–8), with the latter itself able to recognize particular nuclear transport substrates. These include the T cell protein tyrosine phosphatase (9), the yeast transcription factor GAL4 (10), the viral gene products Rev (11, 12) and Rex (13) of human immunodeficiency virus-1 and the human T cell leukemia virus-1, respectively, cyclin B1 (14), and the polypeptide ligand PTH-related protein (PTHrP) (15).

PTHrP was initially discovered as a circulating factor secreted by certain cancers and is responsible for the syndrome of humoral hypercalcemia of malignancy (16). In normal postnatal mammals, PTHrP has not been shown to function as a hormone but is expressed in many normal tissues where it exerts autocrine/paracrine or intracrine actions (16–21). Resemblance to PTH at the amino terminus is sufficient to confer functions similar to those of PTH, which are mediated by the shared PTH/PTHrP receptor and adenylate cyclase activation, such as the promotion of bone resorption and reduction of renal calcium excretion (16, 22). Other roles, such as the regulation of placental calcium transport to the fetus (16, 22, 23), osteoclast inhibition (24), and the control of cell growth and apoptosis (17, 25), have been ascribed to distinct regions of PTHrP.

Apart from being expressed in a cell cycle-dependent manner (26, 27), PTHrP localizes conditionally to the nucleus/nucleolus at G_1 (28) with regulation of PTHrP subcellular localization mediated through phosphorylation by the cyclin-dependent kinases $p33^{cdk2}$ and $p34^{cdc2}$. A key phosphorylation site in regulating PTHrP nuclear localization appears to be T^{85} (28), in the vicinity of an SV40 large T antigen-like NLS ($PGKKKKGK^{93}$). Intriguingly, PTHrP amino acids 67–94, comprising this NLS and amino-terminal flank-

Abbreviations: CLSM, Confocal laser scanning microscopy; FRAP, fluorescence recovery after photobleaching; GFP, green fluorescent protein; GST, glutathione-*S*-transferase; NLS, nuclear localization sequence; PTHrP, PTH-related protein.

ing regions, are recognized with nanomolar affinity by the nuclear transport factor importin β1 rather than by the conventional NLS-binding importin α subunit (15), and PTHrP nuclear import *in vitro* is able to be mediated by importin β1 and the monomeric GTP-binding protein Ran in the absence of importin α. The importance of this nuclear import pathway is indicated by the fact that deletion of the basic residues of the NLS results in complete cytoplasmic localization of PTHrP and concomitant impaired PTHrP-conferred resistance to apoptosis on the part of transfected CFK2 chondrocytes (17). Nuclear PTHrP correlates with an increase in mitogenesis in vascular smooth muscle cells (20) and enhanced IL-8 expression in prostate cancer cells (29). Nuclear/nucleolar uptake of PTHrP is also observed subsequent to internalization of extracellular ligand by osteogenic sarcoma cells expressing the shared PTH/PTHrP receptor (PTH1R) (15).

In the present study, we examine nuclear transport of PTHrP in living cells using a PTHrP-green fluorescent protein (GFP) fusion protein and the technique of fluorescence recovery after photobleaching (FRAP). We show that PTHrP can shuttle in both directions between cytoplasm and nucleus and can resolve the nuclear import process temporally. We demonstrate PTHrP association with β-tubulin *in situ* using several microscopic approaches, as well as *in vitro,* using taxol-polymerized microtubules where, intriguingly, binding of PTHrP was enhanced in the presence of importin β1. Importantly, cells pretreated with the microtubule-disrupting agent nocodazole show significantly reduced fractional return of nuclear and nucleolar fluorescence in FRAP experiments, indicating that PTHrP nuclear/nucleolar transport is dependent on microtubule integrity.

RESULTS

FRAP to Study Nuclear-Cytoplasmic Flux

To characterize the intracellular localization and transport of PTHrP in living cells, a plasmid (pSMR792) was constructed for expression of a GFP-PTHrP (amino acids 1–141) fusion protein (GFP-PTHrP, approximately 45 kDa) lacking the prepro region (-36 to -1) to prevent secretion of the molecule (15); this form is comparable to the nonsecreted form of PTHrP generated through an alternate transcriptional start site (30). Forty-eight hours after transfection, subconfluent UMR 106.01 osteogenic sarcoma cells consistently showed nuclear/nucleolar as well as cytoplasmic localization of GFP-PTHrP when visualized by confocal laser scanning microscopy [CLSM (Fig. 1A, *top left panel*)]. The steady state level of accumulation within the nucleus (Fn/c) and nucleolus (Fnu/c) relative to the cytoplasm was 5.54 $\pm$ 1.0 and 6.92 $\pm$ 1.29 (n = 20), respectively. In contrast, analysis of a control construct of GFP alone [27 kDa (Fig. 1A, *bottom left panel*)] yielded a nuclear to cytoplasmic fluorescence ratio (Fn/c) of 1.13 $\pm$ 0.04 (n = 5), indicative of equilibration of the protein between nuclear and cytoplasmic compartments through simple diffusion.

To compare intracellular movement of GFP-PTHrP to that of GFP as a control, the nucleus of the cell was bleached using the confocal laser at high energy, and the return of fluorescence was then monitored at lower laser energy every 20 sec for up to about 8 min. The recovery of fluorescence to the nucleus/nucleolus of GFP-PTHrP and GFP through transport from the cytoplasm, after the initial pre-/postbleach images is shown in Fig. 1A. Representative quantitative data are shown in Fig. 1B, indicating that the average fractional return of PTHrP to the nucleus and nucleolus was 52.6 $\pm$ 3.1 and 61.4 $\pm$ 4.1% (n = 19), respectively, with $t_{1/2}$ values of 21.6 $\pm$ 3.1 and 23.8 $\pm$ 3.4 sec (n = 19), respectively. When photobleaching of a volume of the cytoplasm equivalent to that in the bleach of the nucleus was performed, fluorescence due to GFP-PTHrP was observed to relocate to the cytoplasm with a consequent fall in nuclear and nucleolar fluorescence (data not shown); the rate of export from the nucleus was about 3-fold slower than that of nuclear import (see also Ref. 42). Experiments on cells expressing GFP alone (*e.g*. Fig. 1B, *bottom panels*) indicated almost 5-fold slower rates of return of nuclear fluorescence ($t_{1/2}$ of 106 $\pm$ 8.3, n = 3), representing the difference between simple diffusion (GFP) and NLS-facilitated transport (GFP-PTHrP). Together, these data imply that PTHrP fluxes continuously between the nucleus and cytoplasm, with transport in the import direction being faster (42).

Localization of PTHrP to the Microtubule Network

Although we have previously observed colocalization of PTHrP with cytoskeletal structures, we had not been able to demonstrate colocalization with actin filaments (28). Accordingly, we used high-resolution fluorescence imaging using two-photon laser excitation (31) to re-examine GFP-PTHrP subcellular localization, results clearly indicating that, in addition to predominant nucleolar and nuclear localization, cytoplasmic PTHrP was observed associated with distinct filamentous structures (Fig. 2). Because two-photon excitation is not ideally suited to colocalization studies, we used more conventional CLSM and coimmunofluorescence to determine whether the filamentous structures with which PTHrP appeared to associate were microtubules. Coimmunofluorescence of endogenous PTHrP and microtubules (Fig. 3A), as well as colocalization of GFP-PTHrP expressed in transiently transfected cells with microtubules detected using an anti-β-tubulin antibody and Texas Red-labeled secondary antibody (Fig. 3B), was performed; results from both approaches supported the idea that PTHrP colocalized with microtubules. Predominant PTHrP localization in the nucleus/nucleolus was evident, as was the localization of cytoplasmic PTHrP to filamen-

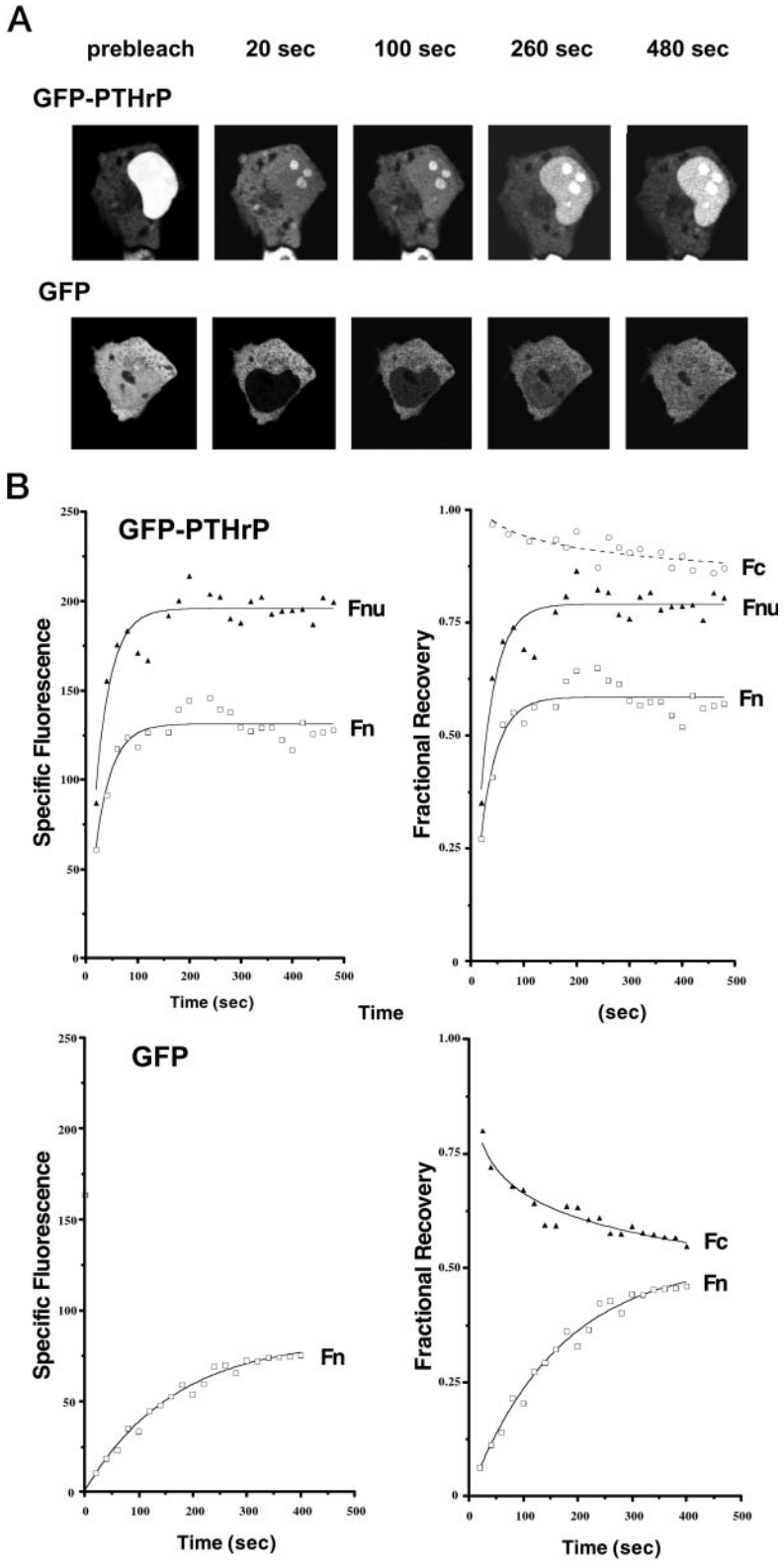

Fig. 1. Results for FRAP of UMR 106.01 Cells Expressing GFP-PTHrP or GFP Alone

A, Visualization using CLSM of the recovery with time of fluorescence into the nucleus after photobleaching, performed as described in *Materials and Methods*, for GFP-PTHrP (*top*) and GFP (*bottom*). A movie of the former experiment is available at *http://jcsmr.anu.edu.au/dbmb/jans/lam/frap/ (Fig.1.avi).* B, Quantitation of the recovery with time of fluorescence into the nucleus/nucleolus after photobleaching for GFP-PTHrP (*top panels*) or GFP (*bottom panels*) expressed in terms of specific nuclear (Fn) or nucleolar (Fnu) fluorescence (*left panels*), or fractional recovery of Fn, Fnu, or Fc (cytoplasmic fluorescence) (*right panels*).

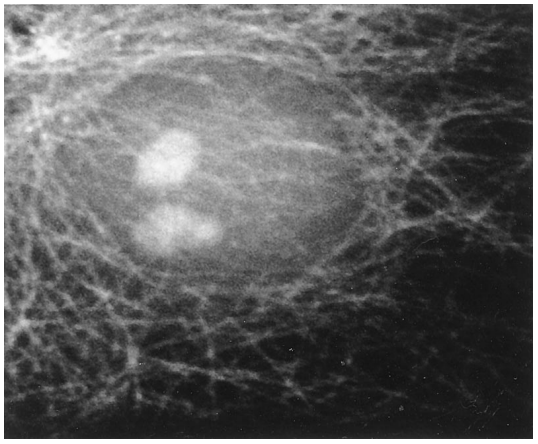

Fig. 2. Visualization of Subcellular Localization of GFP-PTHrP in UMR 106.01 Transfected Cells Using Two-Photon Excitation (100× Objective)

Imaging was performed as described in *Materials and Methods* section.

tous, microtubule-like structures (Fig. 3); colocalization with β-tubulin was clearly evident when *green* and *red* channel images were merged (Fig. 3, *right panels*). Studies (Fig. 3B, *middle panels*) performed using cells pretreated with nocodazole, a specific microtubule-disrupting agent that binds to microtubule subunits and prevents heterodimers from repolymerizing, indicated that concomitant with the disruption of microtubule structure, filamentous localization of cytoplasmic GFP-PTHrP was absent (Fig. 3B; *middle panels*); limited colocalization in the GFP/Texas Red-merged image (not in filaments; Fig. 3B, *middle right panel*) was observed, consistent with the association of PTHrP with depolymerized β-tubulin. Control experiments using cells transfected to express GFP (Fig. 3B, *bottom panels*) indicated a lack of filamentous structure localization and lack of colocalization with β-tubulin (Fig. 3B, *bottom right panel*); thus, these results strongly implicated the specific nature of PTHrP association with microtubules.

To confirm these observations, transiently transfected GFP-PTHrP expressing UMR 106.01 cells were microinjected with rhodamine-labeled tubulin. Forty five minutes after injection, cells that had formed rhodamine-labeled microtubules were subjected to FRAP analysis, and both GFP-PTHrP and rhodamine-labeled microtubules were visualized through separate channels on a CLSM (Fig. 4A). Quantitation of GFP-PTHrP nuclear import in these cells showed no difference in the rate or extent of transport between microinjected and nonmicroinjected cells, indicating that the cells were not damaged during the microinjection procedure (Fig. 4B). There was no rhodamine-tubulin in the nuclei of these cells and no movement of rhodamine-tubulin into the nucleus for the duration of the experiment (Fig. 4B). As expected, not all the microinjected rhodamine-tubulin was assembled into microtubules, but careful analysis of the cytoplasm (highlighted by the *white arrows* in Fig. 4A, i and ii) revealed that GFP-PTHrP colocalized with rhodamine-labeled microtubules (*yellow* in the merged images); in some cases, it was possible to discern the movement of PTHrP (seen as *yellow spots*) along the microtubules toward the nucleus during the course of the experiment (data not shown).

Association of PTHrP to the Microtubule Network Is Enhanced in the Presence of Importin β1

It has previously been shown that plant importin α is able to interact with microtubules in an NLS-dependent fashion (32). To test whether a similar mechanism might operate in a mammalian system for the importin β1-mediated import substrate PTHrP, a microtubule association assay was used. Taxol-assisted microtubule formation was performed *in vitro*, followed by the addition of combinations of PTHrP, importins, and UMR106.01 total cell lysate, followed by incubation for 30 min. The microtubule/protein mixtures were then spun through a glycerol gradient, and the resulting microtubule pellet was analyzed for the presence of PTHrP by SDS-PAGE and Western blotting (Fig. 5). First, exogenously added PTHrP was found to associate with microtubules in the presence of total cell lysate, which contained all the necessary components for nuclear import (Fig. 5A, lane 3), with endogenous PTHrP in the cell lysate also found to associate with the microtubules (Fig. 5A, lane 2). Addition of recombinant importin β1 caused the strongest association of PTHrP to the microtubules (Fig. 5A, lane 7). As negative controls, cell lysate or protein alone (not mixed with preformed microtubules) was spun through the glycerol cushion and analyzed by Western blotting. PTHrP alone (Fig. 5A, lane 10) or in cell lysates (Fig. 5A, lane 9) did not pellet through the glycerol cushion; nor did importin α or β1 (Fig. 5A, lanes 12 and 11, respectively). Whole-cell lysate run on the same blot (Fig. 5A, lane 13) demonstrated functionality of the anti-PTHrP antibody.

To test whether PTHrP alone could bind to microtubules in the absence of cell lysate, recombinant PTHrP was added (Fig. 5B, lane 1), its microtubular association being enhanced about 2-fold in the presence of importin β1 (Fig. 5B, lane 2, and Fig. 5D); microtubular association of importin β1 could also be detected (data not shown). In support of its specific requirement for importin β1, and not importin α, for nuclear import (15), addition of importin α did not enhance but rather decreased microtubular association of PTHrP more than 3-fold (Fig. 5B, lane 3, and Fig. 5D). These results indicated that PTHrP associates directly with microtubules, with importin β1 able to enhance this process.

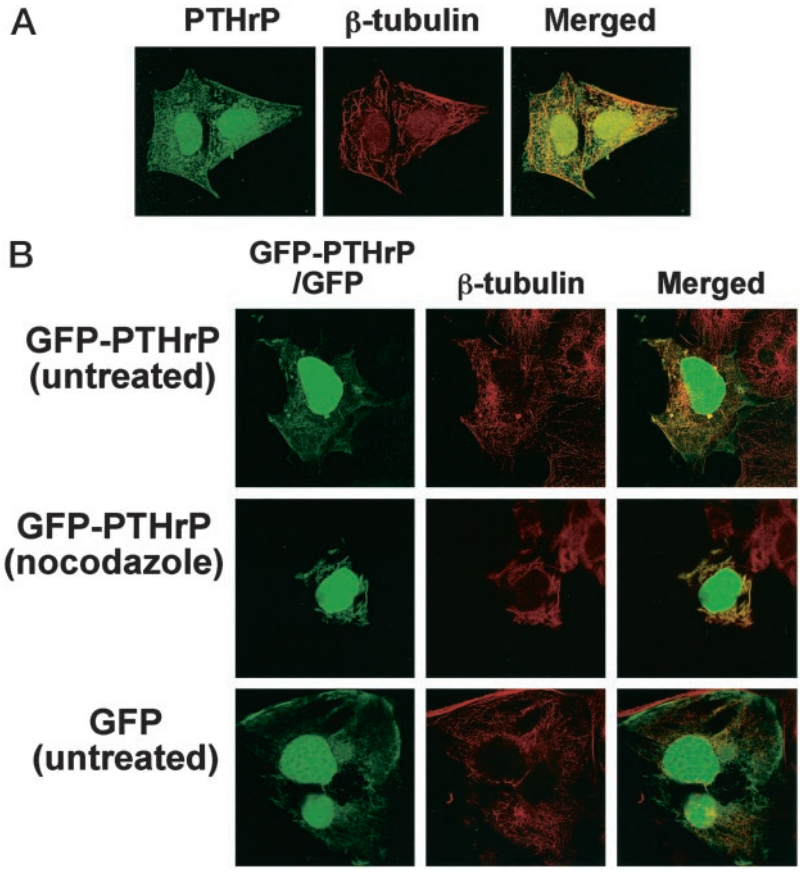

Fig. 3. Colocalization of Endogenous and Transfected PTHrP with Microtubules

A, Immunolocalization of endogenous PTHrP in UMR 106.01 cells was performed using a rabbit anti-PTHrP antibody (Oregon Green-labeled secondary antibody), whereas β-tubulin was detected by immunolocalization using a mouse anti-β-tubulin antibody (rhodamine-labeled secondary antibody). PTHrP (*green*) is shown in the *left* panel, β-tubulin (*red*) in the *middle* panel, and merged images on the *right* with colocalization in *yellow*. Magnification, 2,500×. B, UMR 106.01 cells transfected with GFP-PTHrP (*top* and *middle* panels) or GFP (*bottom* panels) were left untreated (*top* and *bottom* panels), or treated with 10 μg/ml nocodazole for 1 h (*middle*). β-Tubulin was detected by immunolocalization using a mouse anti-β-tubulin antibody (rhodamine-labeled secondary antibody). PTHrP-GFP (*green*) is shown in the *center* panels, β-tubulin (*red*) in the *left* panels, and merged images on the *right* with colocalization in *yellow*. Magnification, 1,200×.

Microtubule Integrity Is Essential for PTHrP Nuclear Import

To test directly whether an intact microtubule network is necessary for nuclear import of PTHrP, transiently transfected cells expressing GFP-PTHrP were pretreated for 60 min with nocodazole, and PTHrP subcellular localization examined by CLSM. Steady state analysis revealed increased levels of nuclear/nucleolar GFP-PTHrP in the treated cells compared with controls (data not shown), indicating reduced nucleocytoplasmic flux for PTHrP. FRAP experiments indicated that nocodazole pretreatment reduced the extent of the return of nuclear/nucleolar fluorescence after photobleaching (29.8 ± 2.1 and 34.8 ± 3.2%, n = 20, for nucleus and nucleolus, respectively; Fig. 6, A and B, and Fig. 7) significantly ($P < 0.0001$) compared with untreated cells (52.6 ± 3.1 and 61.4 ± 4.1%, n = 19, for nucleus and nucleolus, respectively; Fig. 6, A and B and Fig. 7). The $t_{1/2}$ of fluorescence recovery was markedly longer ($t_{1/2}$ of 37.8 ± 7.2 and 42.2 ± 7.6 sec, n = 19, for nuclear and nucleolar fluorescence, respectively) when compared with that of untreated cells (Fig. 7). Similar results were obtained after 24-h treatment with nocodazole (results not shown). Taken together, the results from Figs. 4–7 clearly imply a role for the cytoskeleton and, in particular, the microtubule network in transporting PTHrP toward the nucleus.

DISCUSSION

The technique of FRAP has been used extensively in biological systems to study the lateral mobility of proteins within the plasma membrane (33–37), the nuclear membrane (38), or within organelles (39). In terms of nuclear transport, FRAP had been used together with fluorescent dextrans to determine the diffusion size limit across the nuclear pore complex (40) as well as to

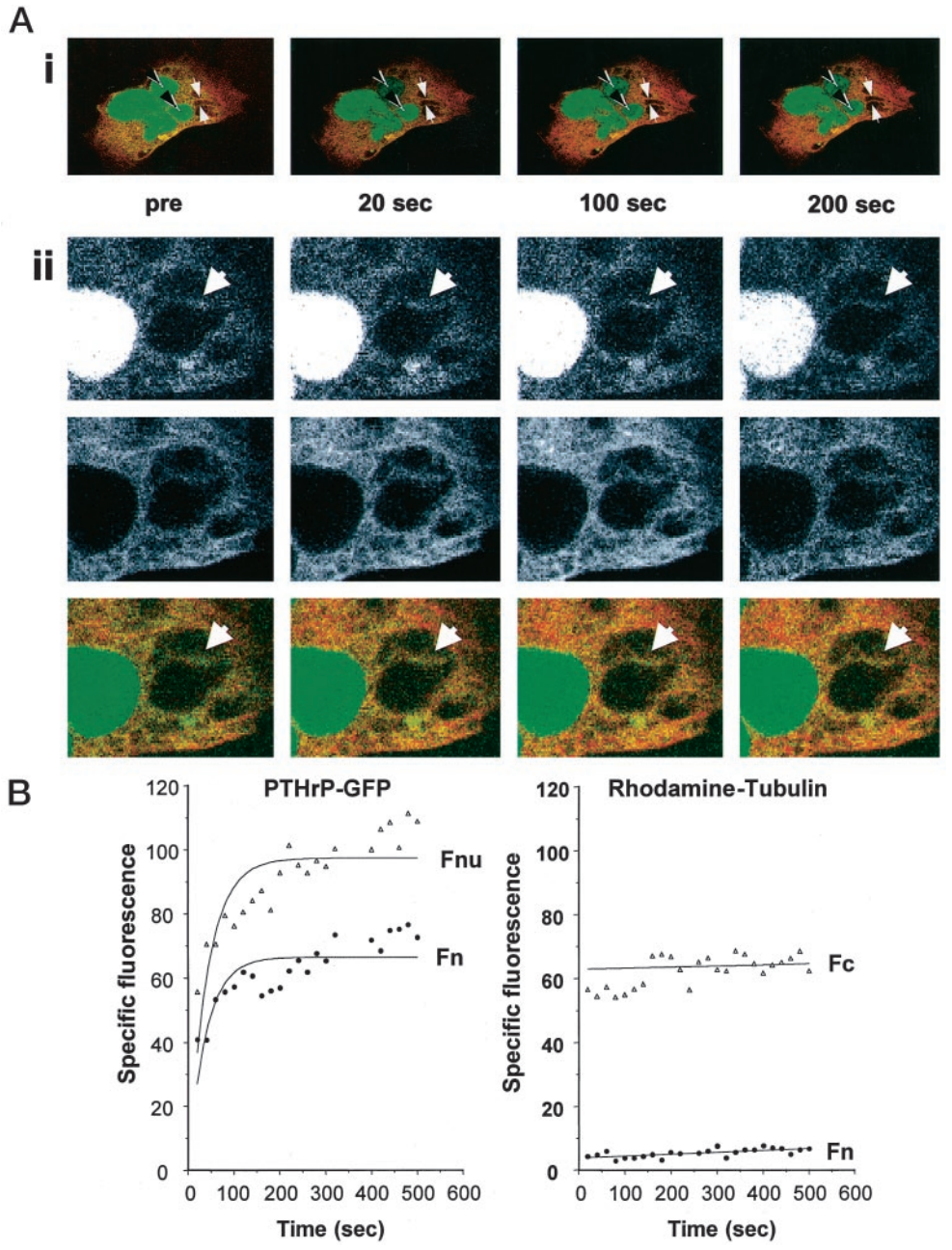

Fig. 4. Visualization of GFP-PTHrP on Rhodamine-Labeled Microtubules in Living Cells Using FRAP

A, UMR 106.01 cells transfected with GFP-PTHrP were microinjected with rhodamine-labeled tubulin and returned to tissue culture for 45 min to enable incorporation into microtubules. Cells were then photobleached (bleach area indicated by the *black arrow*), with the nuclear and nucleolar import visualized (i) as described in the legend to Fig. 1; a movie of this experiment is available at *http://jcsmr.anu.edu.au/dbmb/jans/lam/frap/ (Fig.4i.avi*), with (ii) showing separate channel images of a detail of the same cell, where *green* and *red* channels are the *top* and *middle* series of panels, respectively, and the merged image is shown in the *bottom* panels. Colocalization of GFP-PTHrP and tubulin (*yellow spots* indicating *green* and *red* colocalization) is evident along microtubules (*red*); *white arrows* highlight PTHrP (*yellow dots*) on microtubules; a movie of this is available at *http://jcsmr.anu.edu.au/dbmb/jans/lam/frap/ (Fig.4ii.avi)*. B, Quantitation of the kinetics of return of fluorescence of GFP-PTHrP into the nucleus and nucleolus after photobleaching (*left* panel), performed as described in the legend to Fig. 1. No movement (no increase in Fn and no decrease in Fc) of rhodamine-tubulin into the nucleus is observed (*right* panel).

assess the lateral mobility of nuclear import substrates in the nuclear or cytoplasmic compartments (41). In this study, we use FRAP in conjunction with a GFP-fusion protein for the first time as a means of studying, in living cells, the nucleocytoplasmic flux of a protein for which the nuclear transport mechanism has been delineated (15). This approach has the advantage over conventional nuclear transport assays in that 1) cells

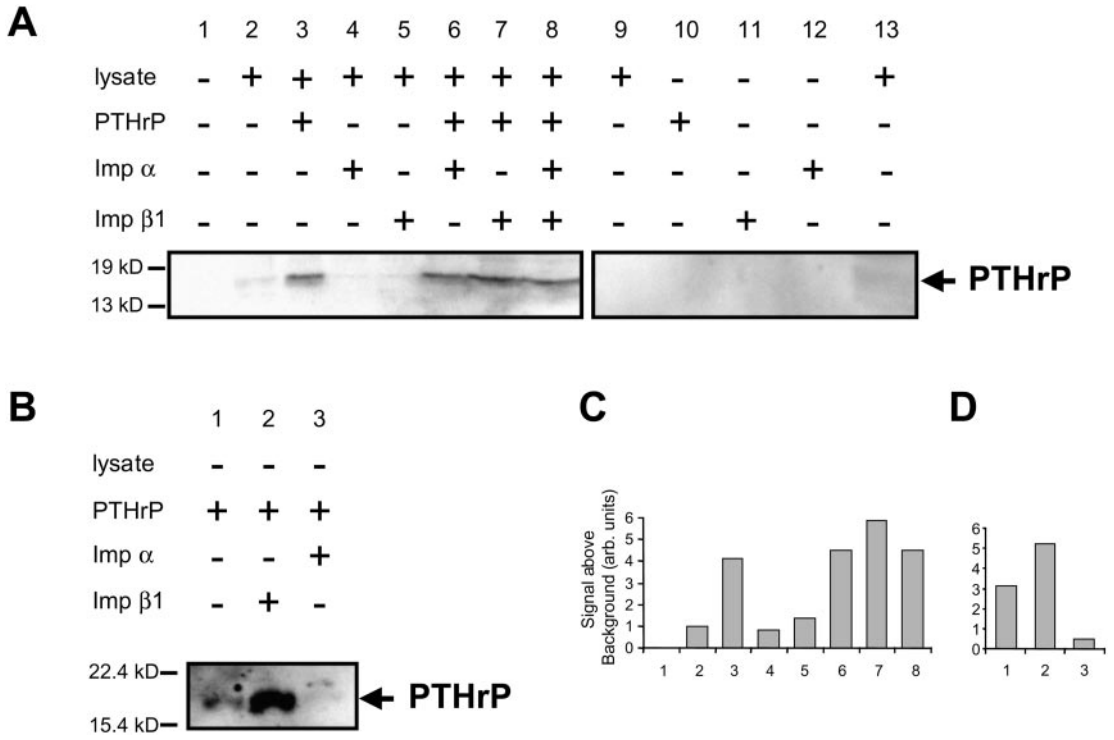

Fig. 5. PTHrP Associates with Microtubules, and Its Association Is Enhanced by Importin β1

Microtubule association was determined by the ability of PTHrP to pellet with the microtubules through a 60% glycerol cushion. The resulting microtubule pellets were analyzed by SDS-PAGE, blotted on a nitrocellulose membrane, and probed using an anti-PTHrP antibody and horseradish peroxidase-coupled secondary antibody, developed using enhanced chemiluminescence, and imaged using a cooled charge-coupled device camera (see *Materials and Methods*). For control experiments, proteins that were not incubated with taxol-stabilized microtubules were subjected to the same protocol as above (lanes 10–12). Microtubules formed in the presence of taxol were incubated in the presence (A) or absence (B) of UMR106.01 cell lysate with combinations of exogenously added PTHrP, importin β1, and importin α (as indicated *below* each lane). As controls, PTHrP, importin β1, and importin α were also added to glycerol cushions and spun (panel A, lanes 9–12). Whole-cell lysates from UMR 106.01 cells (no centrifugation through a glycerol cushion) were used to test the efficacy of the antibody (panel A, lane 13). C, Quantification of data shown in A (lanes 1–8; *left* panel) using ImageGauge software (Fuji Photo Film Co., Ltd.). D, Quantification of data shown in panel B.

are not physically damaged by microinjection, detergent, or mechanical perforation, and 2) that proteins are expressed intracellularly and hence do not have to be introduced exogenously, which allows for the study of their nuclear transport in as physiological a context as possible. The technique is quantitative, enables actual nuclear transport rates to be determined, and permits temporal resolution of the nuclear import process in intact living cells.

The present results suggest that under normal conditions, PTHrP is able to cycle between the nucleus and cytoplasm via the nuclear pore complex. Although nuclear import is mediated by importin β1, based on previous work (15), export of PTHrP is leptomycin B sensitive, implying involvement of the nuclear export receptor CRM1 (42). PTHrP association with cytoskeletal elements has recently been reported (30), and, as shown here for the first time, microtubule integrity clearly plays an important role in PTHrP nuclear import; whether the integral role of the microtubule network in PTHrP nuclear transport relates directly to the role of importin β1, as opposed to that of the importin α/β1 heterodimer in conventional NLS-dependent nuclear protein import, is unclear. The role of microtubules in PTHrP subcellular localization is indicated by the demonstration of colocalization with β-tubulin, the direct visualization of GFP-PTHrP on rhodamine-labeled microtubules after FRAP, and the fact that the microtubule-disrupting agent nocodazole alters the steady state level of PTHrP nuclear/nucleolar accumulation and its nucleocytoplasmic flux. Further, we show that PTHrP is able to bind to *in vitro* polymerized microtubules and that this association is enhanced by importin β1. We have also detected PTHrP in microtubule preparations from mouse brain, testis, and UMR 106.01 cells (data not shown); significantly, importin β1 was also detected in all of these preparations.

Interestingly, the conventional NLS-binding importin α subunit has been shown to associate with microtubules/microfilaments in mammalian cells (43) and tobacco protoplasts (32), as well as with microtubules *in vitro* in an NLS-dependent manner, whereas yeast importin α has also been reported to bind directly to

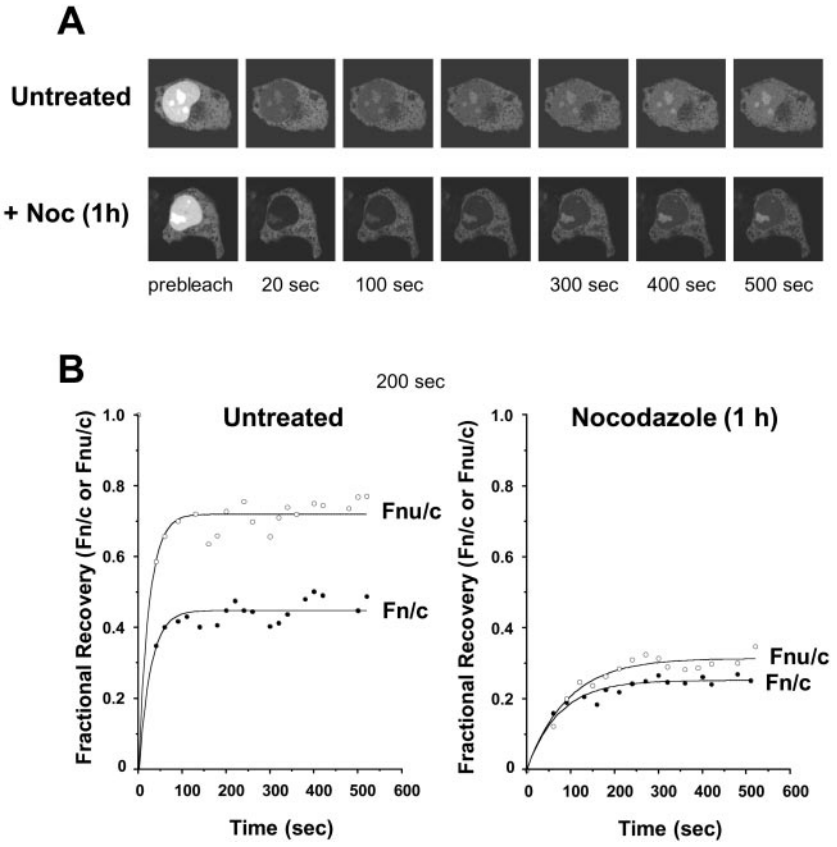

Fig. 6. Results for FRAP Experiments in Untreated and Nocodazole-Treated UMR106.01 Cells Expressing GFP-PTHrP

A, Visualization of the return of fluorescence after photobleaching in control and nocodazole-treated (+ Noc) cells. A movie of this experiment is available at *http://jcsmr.anu.edu.au/dbmb/jans/lam/frap/ (Fig.6.avi).* B, Quantitative analysis from panel A.

the actin-related protein Act2p (44). Microtubule/microfilament association of armadillo repeat-containing proteins, such as catenins and Vac8p (involved in vacuolar protein targeting), has also been reported (32, 45). In the case of several viruses, nuclear import appears to be negatively regulated by association with the actin cytoskeleton (46) or to involve movement along microtubule filaments (47) in analogous fashion to our observations here for PTHrP. Our finding that PTHrP binding to microtubules is enhanced by the presence of its NLS receptor importin β1 is comparable to the NLS-dependent association of plant importin α with microtubules. The close relationship of nuclear import pathways with cytoskeletal components (see Ref. 48) thus may be a general phenomenon of mechanistic importance. The differences in the requirements of individual substrate/importin complexes in terms of binding to microtubules indicate the presence of highly selective mechanisms in transport toward the nuclear pore complex for different NLS-bearing substrates. Intriguingly, preliminary results for FRAP experiments (our unpublished data) on confluent (stationary phase) cells (as opposed to the subconfluent cells exclusively analyzed in this study) are comparable to those for nocodazole-treated cells in terms of a reduced rate of nuclear import and low fractional return of nuclear and nucleolar fluorescence, implying that the importin β1-PTHrP complex interaction with the cytoskeleton may be modulated differentially during cell growth and the cell cycle. The extent to which cell cycle-related phosphorylation at T^{85} of PTHrP (28) may play a role in this is currently being examined.

Although clearly implicated in delaying apoptosis (17) and promoting proliferation (20) in certain cell types, the precise role of PTHrP in the nucleus/nucleolus (49, 50) remains unclear. Poly (G) RNA binding on the part of PTHrP has recently been reported (51), pointing to a possible role of PTHrP, perhaps in conjunction with other proteins, as a nuclear export factor for RNA, consistent with its ability, as shown here, to shuttle between nuclear/nucleolar and cytoplasmic compartments (see above). We have recently shown that treatment of GFP-PTHrP-expressing cells with the RNA-polymerase inhibitor actinomycin D inhibits association of PTHrP with the nucleolus (data not shown), providing further evidence for a role of PTHrP in RNA transport and/or regulation thereof. RNA binding on the part of PTHrP may also contribute to its cytoskeletal association, since a large part of cytoplasmic mRNA appears associated with cytoskeletal elements (52, 53), and nuclear proteins such as the

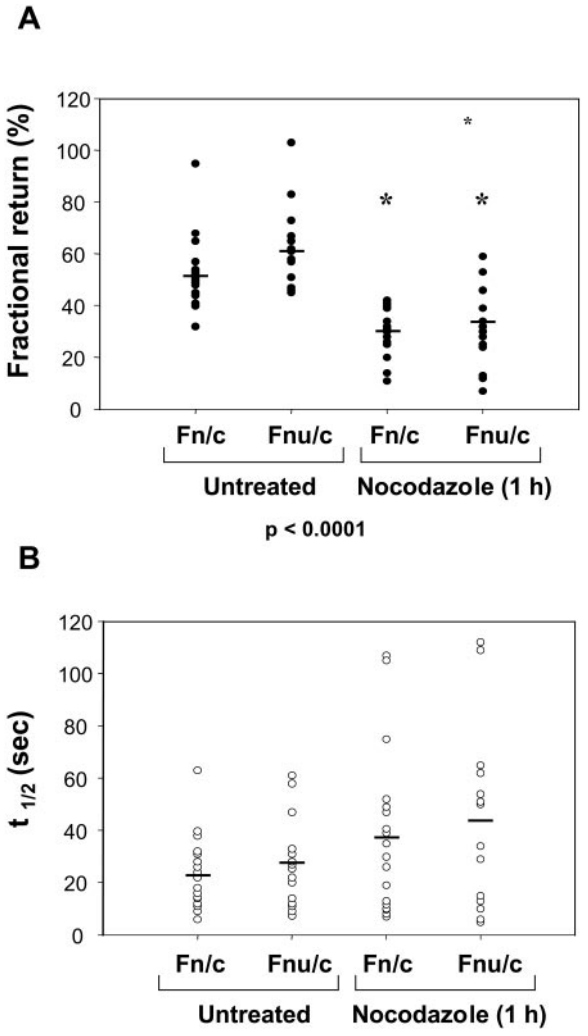

Fig. 7. Pooled Data for the Fractional (A) and Half-Maximal (B) Return of Nuclear and Nucleolar Fluorescence of GFP-PTHrP Subsequent to Nuclear Photobleaching

Values for the maximal fractional return of nuclear fluorescence ($Fn_{500\ sec}/Fn_{prebleach}$) and nucleolus ($Fnu_{500\ sec}/Fnu_{prebleach}$) (*top*) and time in seconds for half-maximal return ($t_{1/2}$) (*bottom*) are shown for untreated and nocodazole-treated cells. * Represents a signifiant ($P < 0.0001$) difference between nocodazole-treated and untreated cells.

mRNA binding protein mrnp41 (52) and Cbf5p, a yeast nucleolar protein that regulates rRNA synthesis (53), have also been demonstrated to associate with the cytoskeleton.

PTHrP was originally discovered as a factor responsible for the syndrome of humoral hypercalcemia of malignancy, with its role as a growth/malignancy factor being implicated by a number of observations (16); MCF-7 and MDA-MD-231 breast cancer cell lines made to overexpress PTHrP, for example, possess increased tumorigenic capacity and metastatic potential (56, 57). The fact (see above) that PTHrP nuclear localization is integral to its function implies that strategies to block PTHrP nuclear localization in cancers overexpressing it could lead to, at least potentially, increased apoptosis and hence reduced tumorigenic potential. The present results, with respect to cytoskeletal and cell cycle control over PTHrP nuclear-cytoplasmic flux, thus may have important application in anticancer therapies, which is the focus of future work in this laboratory.

MATERIALS AND METHODS

Tissue Culture

UMR106.01 rat osteosarcoma cells (56) were maintained in α-MEM supplemented with 10% FBS, at 37 C in 5% $C0_2$ atmosphere.

GFP-PTHrP Fusion Protein Expression Construct

A plasmid expressing GFP fused to the amino terminus of PTHrP(1–141) was generated using oligonucleotide primers as previously described (28). For control experiments in which GFP was analyzed alone, the pEGFP-C1 plasmid (CLONTECH Laboratories, Inc., Palo Alto, CA) was used.

Transfection and Photobleaching Experiments

UMR106.01 cells were passaged onto 22-mm diameter round coverslips for 2 d and then transfected with the GFP-PTHrP-expressing construct using LipofectAMINE (Life Technologies, Inc., Gaithersburg, MD; Ref. 57). Forty eight hours after transfection, the cells were transferred into an open-perfusion microincubator cell chamber (PDMI-2, Medical Systems Corp., Greenvale, NY) and maintained at 37 C in phenol red-free α-modified Eagles medium. GFP-PTHrP expressing cells were identified using CLSM (Bio-Rad MRC-1024; Bio-Rad Microscience, Hemel Hempstead, UK). The CLSM was equipped with a multiline 15-mW Krypton/Argon laser, which allowed for a maximum illumination intensity of approximately 0.3 mW at the point of focus. The cells were visualized ($\times$1.5, zoom; $\times$100, oil immersion lens) by illumination with 10–30% total laser power with excitation at 488 nm. One image (five scans in Kalman mode) was collected before photobleaching, after which an area covering at least 50% of the nucleus was selected by zooming 20-fold. This area was then bleached by removing all barrier filters on the laser to allow for maximum illumination of the area selected for 10 scans (in 8 sec); this did not result in cell death as determined by monitoring the uptake of propidium iodide (data not shown). Images of cells were collected 20 sec after photobleaching, and subsequent images were acquired at 20-sec intervals for about 500 sec using detector and laser settings identical with those used before photobleaching. Because PTHrP binds to nuclear components (15), lateral diffusion from the nonbleached area of the nucleus was assumed to contribute minimally to the return of fluorescence, which was not monitored before 20 sec after photobleaching to avoid this rapid diffusive component; similar approaches have been used and validated with respect to FRAP experiments and the nucleus (39, 40, 60–62). For some experiments, cells were treated with 10 μg/ml nocodazole (Sigma, St. Louis, MO) for 60 min before experimentation. Image analysis was performed using the NIH Image software as described previously (10, 15); autofluorescence was quantitated and subtracted from all other values (Fn, nuclear fluorescence; Fnu, nucleolar fluorescence; Fc, cytoplasmic fluorescence). Fn/c and Fnu/c are the nuclear and nucleolar to cytoplasmic ratios, respectively. FRAP data to calculate the

fractional return of specific fluorescence and $t_{1/2}$ for the return of fluorescence was fitted exponentially as described previously (33, 34, 39, 40).

Two-Photon Excitation Microscopy

High-resolution imaging using two-photon excitation to determine GFP-PTHrP subcellular localization was performed using a Fluoview Confocal Scan system (Olympus Corp., Lake Success, NY) coupled to an Olympus Corp. IX70 Microscope with excitation from a Tsunami/Verdi femtosecond pulsed laser (Spectra-Physics, Mountain View, CA) at 900 nm (31) using a ×100 oil objective.

Microinjection

GFP-PTHrP-expressing UMR 106.01 cells grown on coverslips were microinjected with rhodamine-labeled tubulin (Cytoskeleton, Denver, CO) using a Narshige IM-200 (Narshige, Tokyo, Japan) microinjector as previously described (63). The injected cells were returned to tissue culture for 45 min and then assessed for microtubule formation by CLSM followed by analysis for GFP-PTHrP movement by FRAP as above.

Immunofluorescence

UMR106.01 cells grown on glass coverslips were transfected with the GFP-PTHrP-expressing construct using LipofectAMINE and allowed to express the protein for 24 h. Cells were then left untreated or treated with 10 μg/ml nocodazole for a further 24 h and then fixed with dithiobis succinimidyl propionate (Pierce Chemical Co., Rockford, IL) at 1 mM (in PBS) for 30 min at 37 C, incubated for 5 min with stop solution (0.5% Triton X-100, 1 mM EDTA, 4% polyethylene glycol 6000 in serum-free DMEM), and then incubated for 15 min in 3.2% paraformaldehyde in PBS, pH 7.4, for 15 min at 21 C. The fixed cells were permeabilized and preblocked in 0.1% (wt/vol) BSA and 0.3% (vol/vol) Triton X-100 in PBS for 1 h before incubation with anti-β-tubulin antibody (Roche Molecular Biochemicals, Castle Hill, New South Wales, Australia) overnight at 4 C, followed by a 1-h incubation (21 C) with Texas Red-X-conjugated secondary antibody (Molecular Probes, Inc., Eugene, OR) and mounting with antifade solution (DAKO Corp., Glostrup, Denmark). To colocalize endogenous PTHrP with tubulin, cells were fixed and permeabilized as described above, then coincubated with a polyclonal rabbit anti-PTHrP antibody (R87) specific for the amino terminus (amino acids 1–34) of the molecule together with the anti-β-tubulin antibody, followed by hybridization with Oregon Green-conjugated anti-rabbit and Texas Red-X antimouse conjugated secondary antibodies. Imaging was performed using CLSM. The red and green channels were collected individually to prevent bleed-through of fluorescence, although the iris settings were set such that uniform confocality was achieved. Images were merged using Confocal Assistant (Bio-Rad version 4.02) and prepared for presentation in Corel Photopaint 8 (Corel Corp.).

Protein Expression and Purification

Recombinant PTHrP(1–108) was expressed and purified as previously described (64). Glutathione *S*-transferase (GST)-tagged mouse importin α1 (PTAC58) and GST-tagged mouse importin β1 (PTAC97) were expressed and purified as previously described (65).

Microtubule Association Assays

To polymerize microtubules, 100 μM bovine brain tubulin, in the form of 33% rhodamine-labeled tubulin and 66% unlabeled tubulin made up in general tubulin buffer [80 mM piperazine-*N,N′*-bis(2-ethanesulfonic acid), pH 6.8, 1 mM $MgCl_2$, 1 mM EGTA, and 10% glycerol; Cytoskeleton, Denver, CO], was polymerized in PMGT, which consists of general tubulin buffer, protease inhibitors (Complete, Roche Molecular Biochemicals), 1 mM GTP, and 100 μM taxol (Sigma) at 35 C for 20 min. Polymerized microtubules were then visualized by CLSM.

For microtubule association, 100 μl of combinations of UMR106.01 cell extract, recombinant PTHrP 1–108 (150 μM), GST-tagged mouse importin β (200 μM), and/or GST-tagged mouse importin α (200 μM) were mixed with the polymerized microtubules and incubated at room temperature for 30 min. The samples were carefully layered onto 400 μl of glycerol cushion buffer [80 mM piperazine-*N,N′*-bis(2-ethanesulfonic acid), pH 6.8, 1 mM EGTA, 1 mM $MgCl_2$, 60% vol/vol glycerol, 0.005% chlorohexadine, and 5 nM taxol] and centrifuged at 100,000 × *g* (Beckman TL100 Ultracentrifuge with a TLA-100.3 rotor, Beckman Coulter, Inc., Palo Alto, CA) at 25 C for 45 min. The microtubule pellet was then resuspended in 100 μl of PMGT, and the microtubule population was monitored using CLSM. The association of PTHrP or importin β with microtubules was assessed by running 20 μl of the microtubule preparations on SDS-PAGE gels followed by transfer to a nitrocellulose membrane and detection with an anti-PTHrP rabbit polyclonal antibody (1903) used at 1:5,000 dilution or an antiimportin β1 goat polyclonal antibody (Santa Cruz Biotechnology, Inc., Santa Cruz, CA) used at 1:1,000 dilution followed by a 1-h incubation in a 1:1,000 dilution of a donkey antirabbit or rabbit antigoat horseradish peroxidase-conjugated Ig (Amersham Pharmacia Biotech, Little Chalfont, Buckinghamshire, UK). Blots were developed using ECL Plus Western blotting detection system (Amersham Pharmacia Biotech), and chemiluminescence was detected using a cooled charge-coupled device camera (Fujifilm LAS1000, Fuji Photo Film Co., Ltd., Tokyo, Japan).

Acknowledgments

We thank Ginny Leopold and Elizabeth Allan for help with tissue culture, and Damian Myers for setting up the microincubator cell chamber.

Received February 1, 2001. Accepted October 23, 2001.

Address all correspondence and requests for reprints to: Professor D. A. Jans, c/o Nuclear Signaling Laboratory, Division of Biochemistry and Molecular Biology, John Curtin School of Medical Research, Australian National University, GPO Box 334, Canberra, ACT 2601, Australia. E-mail: David.Jans@med.monash.edu.au.

This work was supported by National Health and Medical Research Council Australia Program Grant 003211 (to T.J.M. and M.T.G.), an Anti-Cancer Council of Victoria Grant (to T.J.M. and M.T.G.), an Australian National University Institute of Advanced Studies bilateral collaborative scheme grant (to D.A.J.), a Rebecca Cooper Foundation Grant (to M.H.C.L. and D.A.J.), and the Chugai Pharmaceutical Company, Tsukuba, Japan (to T.J.M. and M.T.G.). M.L. is a National Health and Medical Research Council of Australia Peter Doherty Fellow.

* These authors contributed equally to this work.

REFERENCES

1. Goerlich D, Kostka S, Kraft R, Dingwall C, Laskey RA, Hartmann E, Prehn S 1995 Two different subunits of importin cooperate to recognize nuclear localization sig-

nals and bind them to the nuclear envelope. Curr Biol 5:383–392
2. Radu A, Blobel G, Moore MS 1995 Identification of a protein complex that is required for nuclear protein import and mediates docking of import substrate to distinct nucleoporins. Proc Natl Acad Sci USA 92:1769–1773
3. Moroianu J, Hijikata M, Blobel G, Radu A 1995 Mammalian karyopherin $\alpha 1\beta$ and $\alpha 2\beta$ heterodimers: $\alpha 1$ or $\alpha 2$ subunit binds nuclear localization signal and β subunit interacts with peptide repeat-containing nucleoporins. Proc Natl Acad Sci USA 92:6532–6536
4. Pemberton LF, Blobel G, Rosenblum JS 1998 Transport routes through the nuclear pore complex. Curr Opin Cell Biol 10:392–399
5. Wozniak RW, Rout WP, Aitchison JD 1998 Karyopherins and kissing cousins. Trends Cell Biol 8:184–188
6. Goerlich D, Kutay U 1999 Transport between the cell nucleus and cytoplasm. Annu Rev Cell Dev Biol 15: 607–660
7. Nakielny S, Dreyfuss G 1999 Transport of proteins and RNAs in and out of the nucleus. Cell 99:677–690
8. Jans DA, Xiao C-Y, Lam MHC 2000 Nuclear targeting signal recognition: a key control point in nuclear transport? Bioessays 22:532–544
9. Tiganis T, Flint AJ, Adam SA, Tonks NK 1997 Association of the T-cell protein tyrosine phosphatase with nuclear import factor p97. J Biol Chem 272:21548–21557
10. Chan CK, Hubner S, Hu W, Jans DA 1998 Mutual exclusivity of DNA binding and nuclear localization signal recognition by the yeast transcription factor GAL4: implications for nonviral DNA delivery. Gene Ther 5:1204–1212
11. Henderson BR, Percipalle G 1997 Interactions between HIV Rev and nuclear import and export factors: the Rev nuclear localisation signal mediates specific binding to human importin-β. J Mol Biol 274:693–707
12. Truant R, Cullen BR 1999 The arginine-rich domains present in human immunodeficiency virus type 1 Tat and Rev function as direct importin β-dependent nuclear localization signals. Mol Cell Biol 19:1210–1217
13. Palmeri D, Malim MH 1999 Importin β can mediate the nuclear import of an arginine-rich nuclear localization signal in the absence of importin α. Mol Cell Biol 19: 1218–1225
14. Moore JD, Yang J, Truant R, Kornbluth S 1999 Nuclear import of Cdk/cyclin complexes: identification of distinct mechanisms for import of Cdk2/cyclin E and Cdc2/cyclin B1. J Cell Biol 144:213–224
15. Lam MHC, Briggs LJ, Hu W, Martin TJ, Gillespie MT, Jans DA 1999 Importin β recognizes parathyroid hormone-related protein with high affinity and mediates its nuclear import in the absence of importin α. J Biol Chem 274:7391–7398
16. Moseley JM, Gillespie MT 1995 Parathyroid hormone-related protein. Crit Rev Clin Lab Sci 32:299–343
17. Henderson JE, Amizuka N, Warshawsky H, Biasotto D, Lanske BM, Goltzman D, Karaplis AC 1995 Nucleolar localisation of parathyroid hormone-related peptide enhances survival of chondrocytes under conditions that promote apoptotic cell death. Mol Cell Biol 15: 4064–4075
18. Martin TJ, Moseley JM, Williams ED 1997 Parathyroid hormone-related protein: hormone and cytokine. J Endocrinol 154(Suppl):S23–S37
19. Philbrick WM, Wysolmerski JJ, Galbraith S, Holt E, Orloff JJ, Yang KH, Vasavada RC, Weir EC, Broadus AE, Stewart AF 1996 Defining the roles of parathyroid hormone-related protein in normal physiology. Physiol Rev 76: 127–173
20. Massfelder T, Dann P, Wu TL, Vasavada R, Helwig JJ, Stewart AF 1997 Opposing mitogenic and anti-mitogenic actions of parathyroid hormone-related protein in vascular smooth muscle cells: a critical role for nuclear targeting. Proc Natl Acad Sci USA 94:13630–13635
21. Roskams T, Desmet V 1997 Parathyroid-hormone-related peptides. A new class of multifunctional proteins. Am J Pathol 150:779–785
22. Martin TJ, Moseley JM, Gillespie MT 1991 Parathyroid hormone-related protein: biochemistry and molecular biology. Crit Rev Biochem Mol Biol 26:377–395
23. Burtis WJ 1992 Parathyroid hormone-related protein: structure, function, and measurement. Clin Chem 38: 2171–2183
24. Fenton AJ, Kemp BE, Hammonds Jr RG, Mitchelhill K, Moseley JM, Martin TJ, Nicholson GC 1991 A potent inhibitor of osteoclastic bone resorption within a highly conserved pentapeptide region of parathyroid hormone-related protein; PTHrP(107–111). Endocrinology 129: 3424–3426
25. Kaiser SM, Sebag M, Rhim JS, Kremer R, Goltzman D 1994 Antisense-mediated inhibition of parathyroid hormone-related peptide production in a keratinocyte cell line impedes differentiation. Mol Endocrinol 8:139–147
26. Okano K, Pirola CJ, Wang HM, Forrester JS, Fagin JA, Clemens TL 1995 Involvement of cell cycle and mitogen-activated pathways in induction of parathyroid hormone-related protein gene expression in rat aortic smooth muscle cells. Endocrinology 136:1782–1789
27. Lam MH, Olsen SL, Rankin WA, Ho PW, Martin TJ, Gillespie MT, Moseley JM 1997 PTHrP and cell division: expression and localization of PTHrP in a keratinocyte cell line (HaCaT) during the cell cycle. J Cell Physiol 173:433–446
28. Lam MHC, House CM, Tiganis T, Mitchelhill KI, Sarcevic B, Cures A, Ramsay R, Kemp BE, Martin TJ, Gillespie MT 1999 Phosphorylation at the cyclin dependent kinases site (Thr85) of parathyroid hormone-related protein negatively regulates its nuclear localization. J Biol Chem 274:18559–18566
29. Gujral A, Burton DW, Terkeltaub R, Deftos LJ 2001 Parathyroid hormone-related protein induces interleukin 8 production by prostate cancer cells via a novel intracrine mechanism not mediated by its classical nuclear localization sequence. Cancer Res 61: 2282–2288
30. Amizuka N, Fukushi M, Oda K, Ozawa H 1998 Nucleolar localisation and extracellular secretion of PTHrP result from alternative translation utilising CTG and ATG codons. Bone 23:S358
31. Schilders SP, Gu M 1999 Three-dimensional autofluorescence spectroscopy of rat skeletal muscle tissue under two-photon excitation. Appl Optics 38:720–723
32. Smith HM, Raikhel NV 1998 Nuclear localisation signal receptor importin α associates with the cytoskeleton. Plant Cell 10:1791–1799
33. Peters R, Peters J, Tews KH, Bahr W 1974 A microfluorimetric study of translational diffusion in erythrocyte membranes. Biochim Biophys Acta 367:282–294
34. Axelrod D, Ravdin P, Koppel DE, Schlessinger J, Webb WW, Elson EL, Podleski TR 1976 Lateral motion of fluorescently labeled acetylcholine receptors in membranes of developing muscle fibers. Proc Natl Acad Sci USA 73:4594–4598
35. Edidin M, Zagyansky Y, Lardner TJ 1976 Measurement of membrane protein lateral diffusion in single cells. Science 191:466–468
36. Jacobson K, Wu E, Poste G 1976 Measurement of the translational mobility of concanavalin A in glycerol-saline solutions and on the cell surface by fluorescence recovery after photobleaching. Biochim Biophys Acta 433: 215–222
37. Schlessinger J, Elson EL, Webb WW, Yahara I, Rutishauser U, Edelman GM 1977 Receptor diffusion on cell surfaces modulated by locally bound concanavalin A. Proc Nat Acad Sci USA 74:1110–1114
38. Ellenberg J, Siggia ED, Moreira JE, Smith CL, Presley JF, Worman HJ, Lippincott-Schwartz J 1997 Nuclear mem-

brane dynamics and reassembly in living cells: targeting of an inner nuclear membrane protein in interphase and mitosis. J Cell Biol 138:1193–1206
39. Partikian A, Ölveczky B, Swaminathan R, Li Y, Verkman AS 1998 Rapid diffusion of green fluorescent protein in the mitochondrial matrix. J Cell Biol 140: 821–829
40. Lang I, Scholz, M, Peters R 1986 Molecular mobility and nucleocytoplasmic flux in hepatoma cells. J Cell Biol 102:1183–1190
41. Rihs HP, Peters R 1989 Nuclear transport kinetics depend on phosphorylation-site-containing sequences flanking the karyophilic signal of the Simian virus 40 T-antigen. EMBO J 8:1479–1484
42. Lam MHC, Henderson B, Gillespie MT, Jans DA 2001 Dynamics of leptomycin B-sensitive nucleocytoplasmic flux of parathyroid hormone-related protein. Traffic 2:812–829
43. Barsony J. Lenherr S, Shih K, Smith CL, Sackett DL 1997 Importin α mediates steroid receptor interaction with microtubules during translocation. Mol Biol Cell 8S:283 (Abstract)
44. Yan C, Liebowitz N, Melese T 1997 A role for the divergent actin gene, ACT2, in nuclear pore structure and function. EMBO J 16:3572–3586
45. Barth AI, Nathke IS, Nelson WJ 1997 Cadhedrins, catenins and APC protein: interplay between cytoskeletal complexes and signaling pathways. Curr Opin Cell Biol 9:683–690
46. Digard P, Elton D, Bishop K, Medcalf E, Weeds A, Pope B 1999 Modulation of nuclear localization of the influenza virus nucleoporin through interaction with actin filaments. J Virol 73:2222–2231
47. Sodeik B, Ebersold MW, Helenius A 1997 Microtubule-mediated transport of incoming herpes simplex virus 1 capsids to the nucleus. J Cell Biol 136:1007–1021
48. Smith HMS, Raikhel NV 1999 Protein targeting to the nuclear pore. What can we learn from plants. Plant Physiol 119:1157–1163
49. Pederson T 1998 Growth factors in the nucleolus? J Cell Biol 143:279–281
50. Jans DA, Hassan G 1998 Nuclear targeting by growth factors, cytokines, and their receptors: a role in signaling? Bioessays 20:400–411
51. Aarts MM, Levy D, He B, Stregger S, Chen T, Richard S, Henderson JE 1999 Parathyroid hormone-related protein interacts with RNA. J Biol Chem 274: 4832–4838
52. Taneja KL, Lifshitz LM, Fay FS, Singer RH 1992 Poly(A) RNA distribution with microfilaments: evaluation by *in situ* hybridization and quantitative digital imaging microscopy. J Cell Biol 119:1245–1260
53. Bassel G, Singer RH 1997 mRNA and cytoskeletal filaments. Curr Opin Cell Biol 9:109–115
54. Kraemer D, Blobel G 1997 mRNA binding protein mrnp 41 localizes to both nucleus and cytoplasm. Proc Natl Acad Sci USA 94:9119–9124
55. Cadwell C, Yoon HJ, Zebarjadian Y, Carbon J 1997 The yeast nucleolar protein Cbf5p is involved in rRNA biosynthesis and interacts genetically with the RNA polymerase I transcription factor RRN3. Mol Cell Biol 17: 6175–6183
56. Guise TA, Yin JJ, Taylor SD, Kumagai Y, Dallas M, Boyce BF, Yoneda T, Mundy GR 1996 Evidence for a causal role of parathyroid hormone-related protein in the pathogenesis of human breast cancer-mediated osteolysis. J Clin Invest 98:1544–1549
57. Thomas RJ, Guise TA, Yin JJ, Elliott J, Horwood NJ, Martin TJ, Gillespie MT 1999 Breast cancer cells interact with osteoblasts to support osteoclast formation. Endocrinology 140:4451–4458
58. Suda N, Gillespie MT, Traianedes K, Zhou H, Ho PW, Hards DK, Allan EH, Martin TJ, Moseley JM 1996 Expression of parathyroid hormone-related protein in cells of osteoblast lineage. J Cell Physiol 166:94–104
59. Hawley-Nelson P, Ciccarone V, Gebeyehu G, Jessee J 1993 LipofectAMINE reagent: a new, higher efficiency polycationic liposome transfection reagent. Focus 15: 73–79
60. Luby-Phelps K, Lanni F, Taylor DL 1985 Behavior of a fluorescent analogue of calmodulin in living 3T3 cells. J Cell Biol 101:1245–1256
61. Seksek O, Biwersi J, Verkman AS 1997 Translational diffusion or macromolecules-sized solutes in cytoplasm and nucleus. J Cell Biol 138:131–142
62. Ostlund C, Ellenberg J, Hallberg E, Lippincott-Schwartz J, Worman HJ 1999 Intracellular trafficking of emerin, the emery-dreifuss muscular dystrophy protein. J Cell Sci 112:1709–1719
63. Jans DA, Jans P 1994 Negative charge at the casein kinase II site flanking the nuclear localization signal of the SV40 large T-antigen is mechanistically important for enhance nuclear import. Oncogene 9:2961–2968
64. Hammonds Jr RG, McKay P, Winslow GA, Diefenbach-Jagger H, Grill V, Glatz J, Rodda CP, Moseley JM, Wood WI, Martin TJ 1989 Purification and characterization of recombinant human parathyroid hormone-related protein. J Biol Chem 264:14806–14811
65. Xiao CY, Hubner S, Jans DA 1997 SV40 large tumor antigen nuclear import is regulated by the double-stranded DNA-dependent protein kinase site (serine 120) flanking the nuclear localization sequence. J Biol Chem 272:2219–22198